European Journal of Radiology 203 (2026) 113024



Contents lists available at ScienceDirect

European Journal of Radiology

journal homepage: www.elsevier.com/locate/ejrad



Research article



Evaluation of standardized uptake value (SUV) and apparent diffusion coefficient (ADC) as prognostic imaging parameters for primary Ewing sarcoma in hybrid 18F-FDG-PET/MRI

Marcel A. Drews [a,*], Aleksandar Milosevic [a], Johannes Florian Schröder [a], Sebastian Zensen [a], Marcel Opitz [a], Lale Umutlu [a], Wolfgang P. Fendler [b], Ken Herrmann [b], Uta Dirksen [c], Benedikt M. Schaarschmidt [a,d]

[a] Institute of Diagnostic and Interventional Radiology and Neuroradiology, University Hospital Essen, German Cancer Consortium (DKTK) Site Essen, Cancer Research Center (NCT) Cologne-Essen, Hufelandstraße 55, 45147 Essen, Germany
[b] Department of Nuclear Medicine, University Hospital Essen, German Cancer Consortium (DKTK) Site Essen, Cancer Research Center (NCT) Cologne-Essen, Hufelandstraße 55, 45147 Essen, Germany
[c] Pediatrics III, University Hospital Essen, German Cancer Consortium (DKTK) Site Essen, Cancer Research Center (NCT) Cologne-Essen, Hufelandstraße 55, 45147 Essen, Germany
[d] Institute of Radiology, Neuroradiology and Interventional Therapy, University of Erlangen-Nuremberg, Medical Campus Upper Franconia, Klinikum Bayreuth, Bayreuth, Germany

ARTICLE INFO

Keywords:
PET-MRI
Ewing Sarcoma
Diffusion Weighted MRI
Imaging biomarkers
Response prediction
Prognosis prediction

ABSTRACT

Purpose: Ewing sarcoma (EwS) is the second most prevalent malignant bone tumour among juvenile patients. Due to its highly malignant character, itis crucial to identify patients with unfavourable courses as early as possible. In this context, integrated 18F-FDG-PET/MRI combines high-contrast morphological information with functional diffusion imaging and metabolic data and thereby provides ADC and SUV_{max}/SUV_{mean} as established parameters for tumour cellularity and metabolic activity in a single examination. Therefore, our study evaluated the use of ADC and SUV_{max}/SUV_{mean} as prognostic parameters for treatment response and overall survival (OS) in this rare entity. .

Methods: In a monocentric retrospective study, patients with histopathologically-proven EwS who underwent 18F-FDG-PET/MRI before therapy start were included .A polygonal ROI was drawn encompassing the entire tumour mass on fused PET/MR images to determine SUV_{max} and SUV_{mean} and copied onto the ADC maps to quantify ADC_{mean} and ADC_{min}. Dependencies between these parameters and Salzer-Kutschik-Scale(SKS) were analysed by Spearman's correlation coefficients and Hazard ratio for OS.

Results: 39 patients (14 female, median age 16yrs[IQR: 11–23]) were evaluated. Strong inverse correlations between SUV_{max} and ADC_{mean}(ρ = -0.709,p < 0.001) and SUV_{mean} and ADC_{mean}(ρ = -0.689,p < 0.001) were observed. Furthermore, moderate correlations between SKS and SUV_{max}(ρ = 0.502,p = 0.009), SUV_{mean}(ρ = 0.389,p = 0.049) and ADC_{mean}(ρ = -0.425,p = 0.03) were seen as well as correlations between OS and SUV_{max}(HR:5.324,95 %-CI 1.065–26.615,p = 0.042) and SUV_{mean}(HR:5.558, 95 %-CI 1.114–27.733,p = 0.037).

Conclusion: Hence, our study demonstrates a strong correlation between metabolic activity(SUV_{max}/SUV_{mean}) and tumour cellularity(ADC) in EwS and proposes SUV_{max} and SUV_{mean} as prognostic markers for neoadjuvant treatment response and OS. ADC_{mean} also correlates inversely with treatment response but calculating ADC_{mean} and SUV_{max}/SUV_{mean} ratios does not improve prognostic value.

Abbreviations: ADC, Apparent diffusion coefficient; CT, Computed Tomography; CTx, Chemotherapy; EwS, Ewing Sarcoma; HR, Hazard ratio; IQR, Interquartile Range; LNM, Lymphnode metastasis; MTV, metabolic tumour volume; mg/dl, milligram/decilitre; OS, overall survival; PET, Positron Emission Tomography; RTx, Radiotherapy; SKS, Salzer Kuntschik Scale; SUV, standardized uptake value; TLG, total lesion glycolysis; 18-F-FDG, 18-Fluor-Desoxy-Glucose.

* Corresponding author at: Institute of Diagnostic and Interventional Radiology and Neuroradiology, University Hospital Essen, Hufelandstrasse 55, 45147 Essen, Germany.

E-mail address: marcelalexander.drews@uk-essen.de (M.A. Drews).

https://doi.org/10.1016/j.ejrad.2026.113024
Received 25 January 2026; Received in revised form 12 April 2026; Accepted 16 June 2026
Available online 16 June 2026
0720-048X/© 2026 The Authors. Published by Elsevier B.V. This is an open access article under the CC BY license (http://creativecommons.org/licenses/by/4.0/).

1. Background

Ewing sarcoma (EwS) is the second most frequent malignant bone tumour among paediatric and juvenile patients with a prevalence of 2.93 cases/100000 in the US and a median age of 15 years at initial diagnosis. Due to its highly malignant character, prompt and accurate diagnosis of this entity is crucial to determine the most suitable treatment approach [1]. Although current multimodal therapy concepts combining chemotherapy and local therapy have improved 5-years overall survival (OS) of EwS patients over the last decades up to 75 % in localised disease, 5-years OS of multi-metastatic disease is still low with 20–25 % [1–4]. Therefore, the availability of prognostic imaging parameters for therapy response or survival prediction would be beneficial to identify patients with unfavourable courses of disease as early as possible.

Current guidelines recommend MRI for local tumour evaluation and whole-body MRI or 18-F-FDG-PET for whole-body staging in sarcoma [5,6]. In this context, the introduction of 18-F-FDG-PET/MRI in clinical practice offers new possibilities by combining the advantages of the high soft-tissue contrast achieved by MRI and metabolic information given by PET [7–10]. Moreover, diffusion weighted imaging (DWI) can deliver additional information regarding tumour cellularity which has been reported to be associated with aggressiveness in sarcoma [11]. In this context, multiple studies have evaluated the prognostic impact of tumour metabolism quantified by SUV and tumour cellularity measured by ADC for various entities [12–14].Here, an inverse correlation between SUV and ADC was shown for different tumours including osseus as well as non-osseus lesions [4,12,15–17]. In pretherapeutic situation, especially high SUV_{max} was associated with high histopathological grading, poor treatment response and a reduced overall survival in different entities including NSCLC, lymphoma or colorectal cancer [14,18–20].

Regarding sarcoma and especially EwS, data evaluating the prognostic impact of SUV and ADC are based on selected studies only [13,21]. Chodyla et al. proposed 18-F-FDG PET/MRI as a feasible tool for therapy response prediction of soft-tissue sarcoma following of isolated limb perfusion in general [22]. Furthermore, they reported a strong correlation between metabolic activity of soft-tissue sarcoma and neoadjuvant treatment response but found no significant correlation between ADC and treatment response [13]. Additionally, Dudeck et al. as well as Byun et al. suggested a further benefit from ADC analysis for therapy evaluation and patient's survival [23,24]. A detailed (subgroup) analysis on EwS is missing in all these studies. Specific studies on EwS solely focus on PET data from PET/CT as prognostic parameters and deliver contradictory results as Jamet et al. reported a correlation between high SUV_{max} and poor prognosis as well as Annovazzi and El-Hennawy who proposed metabolic tumour volume (MTV) and total lesion glycolisis (TLG) as prognostic parameters [25–27]. In contrast to that, Albano et al. did not find a correlation between metabolic data and outcome [28]. In this context, detailed data on the prognostic value of both – ADC and SUV_{max}/SUV_{mean} using integrated 18F-FDG PET/MRI – specifically focussing on EwS are not available yet. Therefore, the aim of our study was to evaluation a possible correlation between ADC and-SUV_{mean}/SUV_{max} in EwS and the use of these as prognostic parameter for therapy response as well as overall survival prediction in this highly malignant entity using a hybrid PET/MRI setup.

2. Methods

2.1. Patients

For this retrospective study, the institutional databases were reviewed to identify patients that received PET/MRI imaging for EwS evaluation between 01.01.2000 and 30.11.2024. Approval by the local ethics committee was obtained and the need for informed consent was waived due to the retrospective nature of this study (application number: 24–11729-BO; approval date: 23.02.2024).

We included only patients who received the PET/MRI within three months prior to the start of any kind of primary tumour therapy. The EwS needed to be histopathologically proven. Additional clinical data regarding patient's age at initial diagnosis, sex, tumour localisation, clinical stage according to the AJCC classification (8th version) at therapy start as well as the selected therapy were examined.

2.2. Reference standard

For evaluation of neoadjuvant chemotherapy response, Salzer-Kuntschik regression scale (SKS) of the resection specimen was used as reference standard (I: no vital tumour cells, II: single vital tumour cells, III: <10 % vital tumour cells, IV: 10–50 % vital tumour cells, V: >50 % vital tumour cells, VI: completely vital tumour) [29]. No response analysis was performed for the primary radiotherapy subgroup. Overall survival was defined as the timespan between initial diagnosis and date of death respectively last clinical visit. Patient's survival data were obtained from clinical database and the corresponding resident registration office.

2.3. PET/MRI acquisition

Before PET/MRI acquisition a body weight-adapted dosage of 18F-fluorodeoxyglucose (18F-FDG) was injected intravenously. Blood glucose levels were measured to ensure values below 150 mg/dl. Calculated activity of administered tracer agent amounted to 208 MBq [IQR: 135–239] 212. The whole-body PET/MRI scans were performed systematically with a delay of 60 min after tracer injection using a 3 Tesla integrated PET/MR system (Biograph mMR, Siemens Healthineers, Germany) in 4–5 bed positions (depending on patients' size) with a PET-data acquisition time of 4 min per bed. In addition, PET-data of the primary tumour were obtained with an acquisition time of 15 min simultaneously with the dedicated MRI scan of the tumour site. For PET image reconstruction the iterative ordered-subset expectation maximization algorithm, 3 iterations and 21 subsets, a Gaussian filter with 4.0 mm full width at half maximum and a 344 × 344 image matrix were used. Attenuation correction was performed with a vendor supplied software solution comprising a four-compartment-model attenuation map (μ-map) calculated from fat-only and water-only datasets, as obtained by Dixon-based sequences as well as an atlas-CT-based bone-anatomy compensation was used. MR images and PET-data were acquired simultaneously. Applied MR sequence protocols depended on the primary tumour localisation and are given in supplementary Tables 1 and 2. Monoexponential ADC-Maps were calculated following image acquisition using the preinstalled software supplied by the vendor on the associated PET/MRI console.

2.4. Image analysis

All images were analysed using the dedicated image processing software SyngoVia (Siemens Healthineers). Axial T1w VIBE post contrast was co-registered with PET images as well as the ADC map. The primary EwS was identified on the co-registered PET/VIBE images and a freehand polygonal region of interest (ROI) was drawn encompassing the biggest extend of the tumour on axial images. The ROI was copied to the same position on the ADC maps (Fig. 2). To avoid pixel void, the ROI was adapted manually. SUV_{max}, SUV_{mean}, ADC_{mean} and ADC_{min} were automatically calculated by SyngoVia and recorded for the primary tumour mass of all patients. SUV_{max}/ADC_{mean} and SUV_{mean}/ ADC_{mean} ratios were calculated manually according to Bruckmann et al. [14]. The ROI analysis was done in a consensus reading session by two radiologists (M.D. with 5 years and B.S. with 12 years of experience in hybrid-imaging).

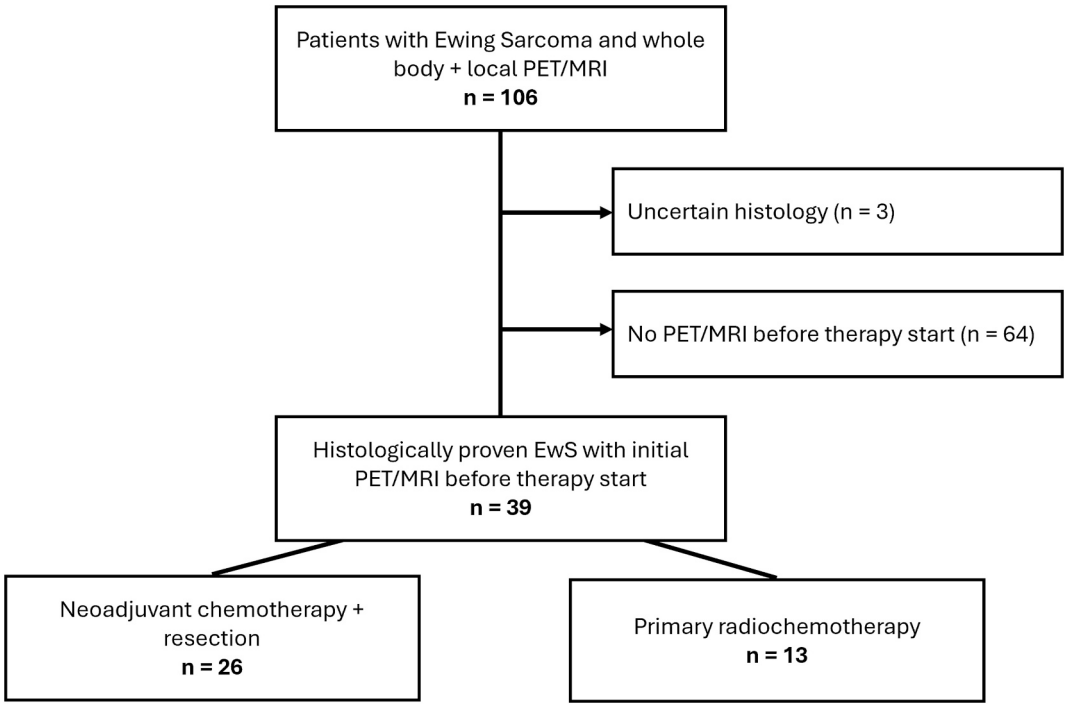


Fig. 1. Flow diagram of included patients.

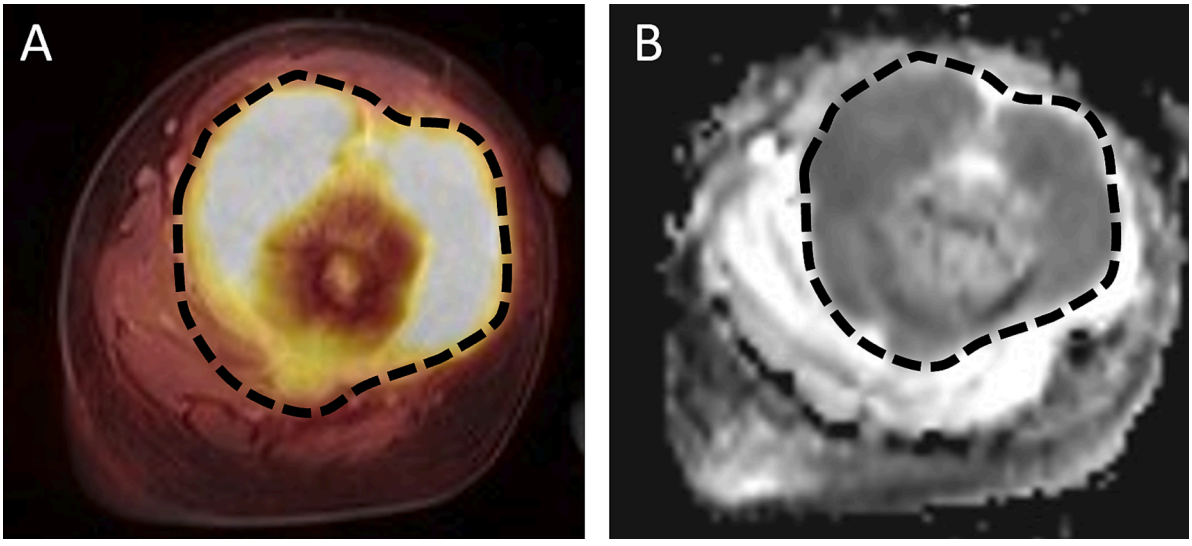


Fig. 2. 10-year-old patient with EwS of the left thigh. Polygonal ROI (dotted line) encompasses the primary tumour mass on PET/VIBE post contrast-MRI fusion image (A) and corresponding ADC-map (B).

2.5. Statistics

Correlation between SUV_{max}, SUV_{mean}, ADC_{mean} and ADC_{min} as well as Salzer Kuntschik Scale were determined using Spearman's correlation coefficient and interpreted according to Cohen (1988) for the neo-adjuvant chemotherapy plus surgery subgroup only. No treatment response analysis was performed for the primary radiochemotherapy subgroup.

To evaluate the correlation of SUV and ADC values with the overall survival, a ROC analysis and Cox regression test was done to determine optimal cut-off values for risk stratification of each measurement. Here, the top-left value of the ROC was used as cut-off [30]. According to these cut-off-values, the cohort was divided into a low- and a high-risk group for each measurement. Kaplan-Meier Curves were plotted and the hazard ratio (HR) as well as the statistical significance based on a log-rank test were computed. Unadjusted p-values < 0.05 were considered significant. All computations were performed using SPSS 29 (IBM Inc., Chicago, IL, USA) and Excel 365 (Microsoft Co., Redmond, WA, USA).

3. Results

3.1. Patient cohort

A total of 106 patients with 18F-FDG-PET/MRI and histopathologically EwS were identified in our database. Three of these patients revealed uncertain histological data and 64 of these already received any kind of treatment (chemotherapy, radiotherapy or surgery) before initial PET/MRI and were excluded. This led to a final study cohort of 39

patients with therapy-naïve EwS (Fig. 1). 26 received neoadjuvant chemotherapy followed by surgical tumour resection and 13 underwent primary radiochemotherapy.

39 patients with histopathologically proven EwS and pretherapeutic PET/MRI were finally included in this study (Table 1). The cohort comprised 35.9 % (14/39) female and 64.1 % (25/39) male patients with a median age at initial diagnosis of 16 years [IQR: 11–23]. Most common primary tumour localisations encompassed the lower extremities with 41 % (16/39), followed by the pelvis 30.8 % (12/39) and lower extremities with 15.4 % (6/39). Uncommon locations included head and thorax with 5.1 % (2/39) each) as well as the spine 2.6 % (1/39). The most common clinical tumour stage at initial diagnosis according to the AJCC classification for bone tumours was IIA with 38.5 % (15/39) followed by IVA and IVB with 17.9 % (7/39) each. 66.7 % (26/39 received neoadjuvant chemotherapy according to the VIDE-scheme and resection of the primary tumour, while 33.3 % (13/39) patients were treated with definitive radiochemotherapy. According to Salzer-Kuntschik regression scale (SKS) of the postoperative specimen in 26 patient, 77 % (20/26) showed a good response to the neoadjuvant treatment (SKS I: 50 % (13/26) SKS II 19.3 % (5/26), SKS III: 7.7 % (2/26)). Poor response (SKS IV + V) was observed in 23 % (6/26) (SKS IV and V: 11.5 % (3/26) each). Median follow-up of the patients was 754 days [IQR: 432–1530]. Regarding subgroups (neoadjuvant chemotherapy + surgery vs. primary radiochemotherapy) demographic data were comparable. Differences were detected in the predominant tumour localisation and AJCC stage. Here, predominant localisation in the surgery group were the lower extremities with 53.8 % (14/26) while the pelvis was the most common localisation in the radiochemotherapy group with 53.8 % (7/13). Patients that underwent surgery were mostly in stage IIA + B (57.7 % [15/26]) and the major part of the radiochemotherapy treated patients was in stage IVA + B (46.2 % [6/13]).

Table 1
Patient data.

	Total cohort	Subgroup (Neoadjuvant chemotherapy + surgery	Subgroup (Primary radiochemotherapy)
Patients	39	26	13
Sex			
female	14 (35.9 %)	9 (34.6 %)	5 (38.5 %)
male	25 (64.1 %)	17 (65.4 %)	8 (61.5 %)
Median age at therapy start (years)	16 [IQR: 11–23]	15 [10.75–23.5]	18 [15–24]
Localisation			
lower extremities	16 (41 %)	14 (53.8 %)	2 (15.4 %)
pelvis	12 (30.8 %)	5 (19.2 %)	7 (53.8 %)
upper extremities	6 (15.4 %)	5 (19.2 %)	1 (7.7 %)
head	2 (5.1 %)	0	2 (15.4 %)
thorax	2 (5.1 %)	2 (7.7 %)	0
spine	1 (2.6 %)	0	1 (7.7 %)
Median of max. tumour diameter (cm)	6.7 [IQR: 5.0–9.2]	3.9 [1.6–6.2]	4.8 [1.0–8.8]
AJCC stage at initial diagnosis	IIA: 15 (38.5 %) IIB: 5 (12.8 %) III: 5 (12.8 %) IVA: 7 (17.9 %) IVB: 7 (17.9 %)	11 (42.3 %) 4 (15.4 %) 3 (11.5 %) 4 (15.4 %) 4 (15.4 %)	4 (30.8 %) 1 (7.7 %) 2 (15.4 %) 3 (23.1 %) 3 (23.1 %)
Salzer-Kuntschik scale:			n/a
1	13 (33.3 %)	13 (50 %)	
2	5 (12.8 %)	5 (19.2 %)	
3	2 (5.1 %)	2 (7.7 %)	
4	3 (7.7 %)	3 (11.5 %)	
5	3 (7.7 %)	3 (11.5 %)	
Median follow up (days)	754 [IQR: 432–1530]	734.5 [IQR: 425–1663]	1045 [IQR: 378–1346]

3.2. Evaluation of metabolic activity and diffusion restriction as potential markers for therapy response prediction

For all 39 patients, median SUV_{max} was 5.1 [IQR: 4.3–6.9] and median SUV_{mean} was 2.7 [IQR: 1.9–3.6] (Table 2). Median ADC_{mean} and median ADC_{min} were 860.7 [IQR: 741.0–1019.7] resp. 305 [IQR: 105–396]. Ratios of SUV_{max}/ADC_{mean} and SUV_{mean}/ADC_{mean} were 0.0060 [0.0038–0.0090] and 0.0032 [0.0017–0.0046].

For the 26 patients who underwent surgery after neoadjuvant chemotherapy median SUV_{max} was 5.2 [IQR: 4.35–7.61] and median SUV_{mean} was 2.7 [1.7–4.5]. Median ADC_{mean} and ADC_{min} in this subgroup were 867.5 [703.7–1018.7] resp. 306.5 [137.25–446.75]. Ratios of SUV_{max}/ADC_{mean} and SUV_{mean}/ADC_{mean} were 0.0062 [0.0039–0.0108] and 0.0032 [0.0017–0.0064].

Using Spearman's correlation coefficient, strong inverse correlations between SUV_{max} and ADC_{mean} ($\rho = -0.709$, $p < 0.001$) as well SUV_{mean} and ADC_{mean} ($\rho = -0.689$, $p < 0.001$) were detected (Table 3). No significant correlations were found regarding SUV_{max} and ADC_{min} ($\rho = -0.157$, $p = 0.34$) or SUV_{mean} and ADC_{min} ($\rho = -0.-0.038$, $p = 0.818$).

Correlating ADC and SUV parameters with SKS as a marker for therapy response revealed a smoderatecorrelation between SUV_{max} and SKS ($\rho = 0.502$, $p = 0.009$) as well as a moderate correlation between SUV_{mean} and SKS ($\rho = 0.389$, $p = 0.049$) (Table 3). Furthermore, a moderate inverse correlation between between ADC_{mean} and SKS was observed ($\rho = -0.425$, $p = 0.03$) while no significant correlation was seen regarding ADC_{min} and SKS ($\rho = -0.229$, $p = 0.26$).

The combined analysis of SUV and DWI using ratios of SUV_{max}/ADC_{mean} as well as SUV_{mean}/ADC_{mean} according to Bruckmann et al. resulted in a slightly weaker but still moderate correlation between SUV_{max}/ADC_{mean} and SKS ($\rho = 0.486$, $p = 0.022$) compared to SUV_{max} and SKS alone. The correlation of SUV_{mean}/ADC_{mean} and SKS was slightly stronger ($\rho = 0.43$, $p = 0.029$) compared to SUV_{mean} and SKS resp. ADC_{mean} and SKS alone.

3.3. Evaluation of metabolic activity and diffusion restriction as potential prognostic markers for OS

Pretherapeutic SUV_{max} as well as SUV_{mean} showed a significant correlation with the OS quantified by a HR of 5.324 (95 % CI 1.065–26.615, $p = 0.042$) for SUV_{max} and 5.558 (95 % CI 1.114–27.733,

Table 2
Median SUV and ADC values as well as their ratios for the total cohort and subgroups.

	All patients (n = 39)	Surgical treatment (n = 26)	Primary radiotherapy (n = 13)
SUV_{max} (median)	5.1 [IQR: 4.3–6.9]	5.2 [IQR: 4.35–7.61]	4.5 [4.2–6.0]
SUV_{mean} (median)	2.7 [IQR: 1.9–3.6]	2.7 [1.7–4.5]	2.4 [2.0–3.1]
ADC_{mean} (median)	860.7 [IQR: 741.0–1019.7]	867.5 [703.7–1018.7]	845.6 [783.8–1246.0]
ADC_{min} (median)	305 [IQR: 105–396]	306.5 [137.25–446.75]	222 [18.5–373.5]
SUV_{max}/ADC_{mean} (median)	0.0060 [0.0038–0.0090]	0.0062 [0.0039–0.0108]	0.0055 [0.0037–0.0071]
SUV_{mean}/ADC_{mean} (median)	0.0032 [0.0017–0.0046]	0.0032 [0.0017–0.0064]	0.0032 [0.0017–0.0041]

Table 3
Correlation between SUV, ADC and their ratios as well as SKS using Spearman's ρ. Significant values are marked with an asterisk.

	ρ	p-value
SUV_{max} vs. ADC_{mean}	−0.709 *	<0.001
SUV_{max} vs. ADC_{min}	−0.157	0.34
SUV_{mean} vs. ADC_{mean}	−0.689 *	<0.001
SUV_{mean} vs. ADC_{min}	−0.038	0.818
SUV_{max} vs. SKS	0.502 *	0.009
SUV_{mean} vs. SKS	0.389 *	0.049
ADC_{mean} vs. SKS	−0.425	0.03
ADC_{min} vs. SKS	−0.229	0.26
SUV_{max}/ADC_{mean} vs. SKS	0.486 *	0.022
SUV_{mean}/ADC_{mean} vs. SKS	0.43 *	0.029

p = 0.037) for SUV_{mean} (Fig. 3 and Table 4). No significant correlations were seen between ADC_{mean} and OS (HR of 2.938 (95 % CI 0.731–11.808, p = 0.138)) as well as ADC_{min} and OS with a HR of 1.867 (95 % CI 0.464–7.517, p = 0.380). Additionally, the SUV_{max}/ADC_{mean} ratio also revealed a significant correlation with the OS showing a HR of 5.246 (95 % CI 1.055–26.097, p = 0.043), but this was slightly worse compared to SUV_{max} alone. The SUV_{mean}/ADC_{mean} ratio was not significantly correlated with the OS showing a HR of 4.332 (95 % CI 0.872–21.515, p = 0.073).

4. Discussion

As EwS is a highly malignant bone tumour predominantly affecting juvenile patients, the early identification of patients at risks for unfavourable courses is key and the availability of imaging parameters would be beneficial in this context. In this retrospective study, we proposed

Table 4
Hazard ratios of SUV, ADC and their ratios as well as OS. Cut-off values were calculated using ROC analysis. Significant values (log-rank test) are marked with an asterisk.

	p-value	HR	HR 95 % CI	Calculated cut-off value
SUV_{max}	0.042 *	5.324	1.065–26.615	5.705
SUV_{mean}	0.037 *	5.558	1.114–27.733	2.83
ADC_{mean}	0.138	2.938	0.731–11.808	811.14
ADC_{min}	0.380	1.867	0.464–7.517	210.5
SUV_{max}/ADC_{mean}	0.043 *	5.246	1.055–26.097	0.00684
SUV_{mean}/ADC_{mean}	0.073	4.332	0.872–21.515	0.00340

SUV_{max}, SUV_{mean} and ADC_{mean} as potential prognostic imaging markers for neoadjuvant chemotherapy response and overall survival in primary EwS using hybrid PET/MRI for the first time.

Initially, we could demonstrate a strong inverse correlation between SUV_{max} and SUV_{mean} with ADC_{mean}. Furthermore, these three parameters show a significant correlation with postoperative SKS proposing these as potential prognostic markers for neoadjuvant chemotherapy response in EwS, while SUV_{max} and SUV_{mean} also show a significant correlation with the OS.

Various cancer entities including sarcoma are characterized by an increased metabolic activity due to high mitosis rates. In this context, SUV of 18F-FDG-PET is a well-established marker for metabolic tissue activity. On the other hand, malignant tumours commonly show a high cellularity. This can be determined in MRI by using DWI. Here, high cellularity results in a restricted diffusion of water molecules and can be quantified using ADC [15,31]. As various studies have demonstrated, increased metabolic activity in tumours is associated with higher

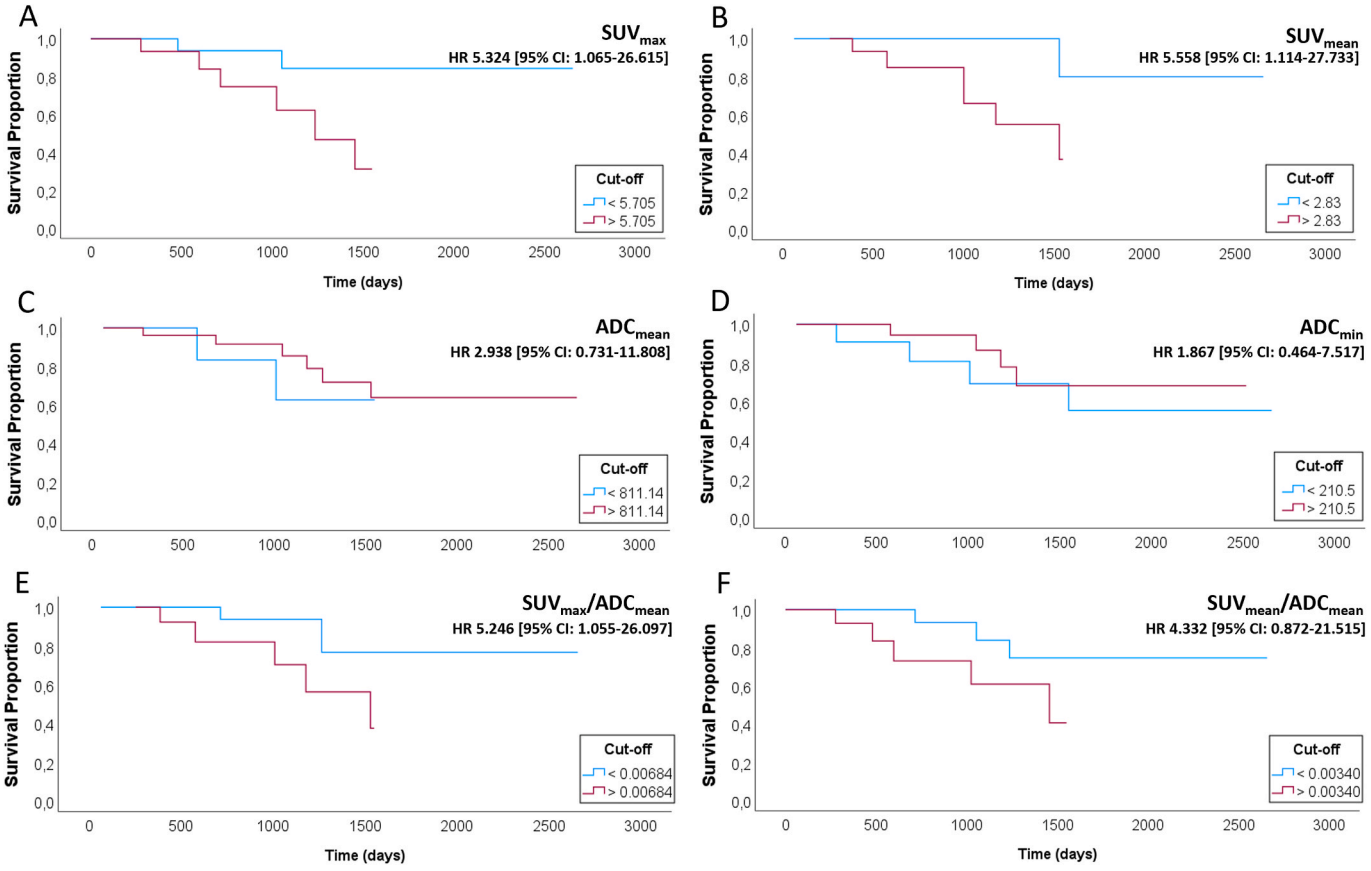


Fig. 3. Kaplan-Meier Curves of SUV_{max} (A), SUV_{mean} (B), ADC_{mean} (C), ADC_{min} (D), SUV_{max}/ADC_{mean} (E) as well as SUV_{mean}/ADC_{mean}. Survival proportion against time in days are plotted in each diagram. The study cohort is divided into a low risk (blue) and a high risk (red) group. Cut-off values are presented in the lower right corner.

cellularity measurable by an inverse correlation between SUV and ADC [32,33]. But data regarding ADC/SUV correlation in soft-tissue sarcomas and especially EwS are scarce and are often based on individual PET/CT and MRI [13]. Here, integrated PET/MRI combines both – metabolic and diffusion data – in a single examination allowing a highly accurate coregistration due to simulataneous acquisition potentially superior to separate MRI and PET/CT [34].

With this study, we could demonstrate a strong inverse correlation between SUV_{max} as well as SUV_{mean} and ADC_{mean} reflecting a relation between high glucose metabolism and increased cellular density in EwS for the first time using a combined PET/MRI setup. In this context, high metabolic tumour areas have been shown to be associated with higher aggressiveness and high histopathological grading proposing these as targets for biopsy, but currently, initial pre-biopsy imaging of local EwS is commonly based on MRI alone without PET component [21,35,36]. Therefore, the demonstrated inverse correlation between SUV and ADC underlines that tumour areas with low ADC_{mean} values should preferably be chosen for biopsy to hit the most aggressive tumour parts as it has been stated for other tumour entities without need of complementary PET data [21,32].

Additional evaluation of ADC_{min} did not reveal significant correlations with SUV_{max}/SUV_{mean} in our study. This could be explained by its higher susceptibility to artifacts. Other studies reported already, that even slight signal magnitude variations under different b-values as well as calcifications may result in very low ADC values including zero which do not reflect the true tumour characteristics and cannot always be excluded by adjusting the drawn ROI[32,37]. Hence, ADC_{mean} is suggested as more robust.

Furthermore, multiple studies have evaluated SUVmax/SUVmean as well as ADC as imaging parameters for therapy response and OS in different entities including soft-tissue sarcomas[17,22,23,38,39]. In selected studies, 18-F-FDG PET/MRI was proposed as a feasible tool for therapy response prediction of soft-tissue sarcoma showing a strong correlation between metabolic activity and neoadjuvant treatment response but lacking EwS subgroup analysis [13,22]. Regarding EwS, specific PET/MRI data is missing as available studies that report the prognostic value of PET parameters including SUV_{max}, TLC and MTV for EwS outcome are solely PET/CT-based [26,27,40–42]. Additionally, single studies also indicate a prognostic value of ADC for chemotherapy response, but this is based on MRI only [43]. Therefore, our study is the first evaluating SUV_{max}/SUV_{mean} as well as ADC from integrated 18F-FDG PET/MRI in the context of prognosis prediction in EwS.

With this study, a strong correlation between SUV_{max} as well as SUV_{mean} and neoadjuvant chemotherapy response evaluated by SKS has been reported for the first time in primary therapy-naïve EwS indicating increased metabolic activity of the primary tumour to be less beneficial for treatment response. Additionally, also higher cellularity quantified by ADC_{mean} shows an inverse correlation with SKS. This is in line with previously considered findings by Chodyla et al. – who reported a correlation between SUV and ADC and treatment response of soft-tissue sarcomas under limb perfusion – and Byun et al. who correlated ADC and SUV from separated PET/CT and MRI with SKS in osteosarcoma [22,24]. Moreover, Bruckmann proposed ratios of SUV_{max}/ADC_{mean} resp. SUV_{mean}/ADC_{mean} to improve prognostic value [14]. We could not verify this for EwS as the correlation of SUV_{max}/ADC_{mean} with SKS was slightly weaker than SUVmax and SKS alone, while on the other hand the correlation between SUV_{mean}/ADC_{mean} and SKS was slightly stronger than ADC_{mean} alone. This leads to the conclusion that SUV_{max} shows the strongest correlation with SKS and the SUV/ADC ratios do not add further prognostic value for EwS treatment response prediction.

Regarding OS, only SUV_{max} and SUV_{mean} showed a significant correlation with. ADC_{mean} and ADC_{min} did not correlate significantly and neither added addition prognostic value with regard to the SUV/ADC ratios. This is in line with studies on other entities including NSCLC, while specific data on EwS are missing [17]. All in all, the independence of these parameters indicates that multiparametic PET/MRI is not superior to PET/CT alone in the prediction of therapy response or OS. As SUV_{max} and SUV_{mean} show a significant correlation with both – neoadjuvant treatment response as well as OS – these appear to be superior to ADC_{mean}.

This study also has limitations. First of all, the total patient number of 39 is low which does not allow further subgroup analysis – especially with regard to initial AJCC tumour stage. As operated patients were predominantly in a lower stage than the radiochemotherapy patients, this could have influenced the analysis. But due to the small subgroup size and lacking a robust reference standard for primary radiochemotherapy, treatment response evaluation could only be performed for the neoadjuvant chemotherapy plus surgery group. Therefore, further analyses in a larger cohort are recommended for the future. Nevertheless, the present study represents to our knowledge the biggest cohort to evaluate correlations between functional MRI and PET in this rare tumor entity, but our findings could be further evaluated in multicenter study with more patients Furthermore, ADC measurements – especially ADC_{min} – are affected by artifacts. Especially, automatic software-based segmentation of the tumour can cause pixel void of areas without any signal and lead to more inconsistent data. Therefore, the ROIs were drawn manually and adapted on the ADC maps to minimize pixel void. Nevertheless, manual segmentation is also a methodical limitation as it could be biased by the investigator. To minimize this bias, the ROI-analysis was done in a consensus reading session by two radiologists. In this context,volumetric histogram-based ADC evaluation has been proposed to improve accuracy and should be evaluated in future studies [44,45]. Additional PET parameters including MTV and TLG could also be evaluated. Over the last years, iterative improvements of attenuation correction in PET/MRI have been made which could have had a minor impact on the SUV. However, since our data are in line with the literature, this can be disregarded in our study [17].

5. Conclusion

In conclusion, our study proposes SUV_{max}, SUV_{mean} and ADC_{mean} as potential prognostic imaging parameters for neoadjuvant chemotherapy response of therapy-naïve EwS using a hybrid 18F-FDG-PET/MRI as a single examination setup. Additionally, SUV_{max} and SUV_{mean} could further be used as prognostic markers for OS, while neither ADC alone nor ratios of SUV and ADC add complementary prognostic value. Therefore, hybrid multiparametric 18F-PET/MRI is not superior to PET/CT or MRI alone in therapy response or OS prediction of EwS.

Ethics approval and consent to participate.

Approval by the local ethics committee was obtained and the need for informed consent was waived due to the retrospective nature of this study (application number: 24–11729-BO; approval date: 23.02.2024).

Consent for publication

Not applicable.

Availability of data and material.

The datasets used and/or analysed during the current study are available from the corresponding author on reasonable request.

Benedikt M. Schaarschmidt received a research grant from PharmaCept GmbH for an investigator-initiated study not related to this paper, a travel grant from Bayer AG and speaker and is a speaker for AstraZeneca, Boston Scientific and Siemens Healthineers.

Funding.

Marcel Drews received funding by the Junior Clinical Scientist Program at the University of Essen Medical School to carry out this project.

Benedikt M. Schaarschmidt received a research grant from PharmaCept GmbH for an investigator- Wolfgang P. Fendler reports fees from SOFIE Bioscience (research funding), Janssen (consultant, speaker), Perceptive (consultant, image review), Bayer (consultant, speaker, research funding), Novartis (speaker, consultant), Telix (speaker), GE Healthcare (speaker, consultant), Eczacıbaşı Monrol (speaker), Abx (speaker), Amgen (speaker, research funding), Urotrials (speaker), Lilly (consultant), AstraZeneca (research funding) outside of the submitted

work.

CRediT authorship contribution statement

Marcel A. Drews: . **Aleksandar Milosevic:** Writing – review & editing, Validation, Investigation. **Johannes Florian Schröder:** Writing – review & editing, Validation, Investigation. **Sebastian Zensen:** Writing – review & editing, Validation. **Marcel Opitz:** Writing – review & editing, Validation. **Lale Umutlu:** Writing – review & editing, Validation. **Wolfgang P. Fendler:** Writing – review & editing, Validation. **Ken Herrmann:** Writing – review & editing, Supervision, Conceptualization. **Uta Dirksen:** Writing – review & editing, Supervision, Conceptualization. **Benedikt M. Schaarschmidt:** Writing – review & editing, Validation, Supervision, Conceptualization.

Declaration of competing interest

The authors declare that they have no known competing financial interests or personal relationships that could have appeared to influence the work reported in this paper.

Acknowledgements

The data of 11 patients presented in this study were already published by Chodyla et al. in a pilot study on therapy response assessment in patiens with Ewing's sarcoma using PET/MRI [10].

This study is listed within the framework of the PET-MR Registry (https://petmr-registry.com). The PET-MR Registry is funded by the Deutsche Forschungsgemeinschaft (DFG) - 441832615.

Appendix A. Supplementary data

Supplementary data to this article can be found online at https://doi.org/10.1016/j.ejrad.2026.113024.

Data availability

Data will be made available on request.

References

[1] S.K. Zollner, J.F. Amatruda, S. Bauer, S. Collaud, E. de Alava, S.G. DuBois, J. Hardes, W. Hartmann, H. Kovar, M. Metzler, D.S. Shulman, A. Streitburger, B. Timmermann, J.A. Toretsky, Y. Uhlenbruch, V. Vieth, T.G.P. Grunewald, U. Dirksen, Ewing Sarcoma-Diagnosis, Treatment, Clinical challenges and Future Perspectives, J. Clin. Med. 10 (8) (2021).

[2] B. Brennan, L. Kirton, P. Marec-Berard, N. Gaspar, V. Laurence, J. Martin-Broto, A. Sastre, H. Gelderblom, C. Owens, N. Fenwick, S. Strauss, V. Moroz, J. Whelan, K. Wheatley, Comparison of two chemotherapy regimens in patients with newly diagnosed Ewing sarcoma (EE2012): an open-label, randomised, phase 3 trial, Lancet 400 (10362) (2022) 1513–1521.

[3] R. Ladenstein, U. Potschger, M.C. Le Deley, J. Whelan, M. Paulussen, O. Oberlin, H. van den Berg, U. Dirksen, L. Hjorth, J. Michon, I. Lewis, A. Craft, H. Jurgens, Primary disseminated multifocal Ewing sarcoma: results of the Euro-EWING 99 trial, J. Clin. Oncol. 28 (20) (2010) 3284–3291.

[4] J. Grueneisen, K. Beiderwellen, P. Heusch, P. Buderath, B. Aktas, M. Gratz, M. Forsting, T. Lauenstein, V. Ruhlmann, L. Umutlu, Correlation of standardized uptake value and apparent diffusion coefficient in integrated whole-body PET/MRI of primary and recurrent cervical cancer, PLoS One 9 (5) (2014) e96751.

[5] A. Gupta, M.S. Dietz, R.F. Riedel, A. Dhir, S.C. Borinstein, M.S. Isakoff, J.M. Aye, N. Rainusso, A.E. Armstrong, S.G. DuBois, L.M. Wagner, J.M. Rosenblum, S. Cohen-Gogo, C.M. Albert, S. Zahler, R. Chugh, M. Trucco, Consensus recommendations for systemic therapies in the management of relapsed Ewing sarcoma: a report from the National Ewing Sarcoma Tumor Board, Cancer 130 (23) (2024) 4028–4039.

[6] S.J. Strauss, A.M. Frezza, N. Abecassis, J. Bajpai, S. Bauer, R. Biagini, S. Bielack, J. Y. Blay, S. Bolle, S. Bonvalot, I. Boukovinas, J. Bovee, K. Boye, B. Brennan, T. Brodowicz, A. Buonadonna, E. de Alava, A.P. Dei Tos, X. Garcia Del Muro, A. Dufresne, M. Eriksson, F. Fagioli, A. Fedenko, V. Ferraresi, A. Ferrari, N. Gaspar, S. Gasperoni, H. Gelderblom, F. Gouin, G. Grignani, A. Gronchi, R. Haas, A.B. Hassan, S. Hecker-Nolting, N. Hindi, P. Hohenberger, H. Joensuu, R.L. Jones, C. Jungels, P. Jutte, L. Kager, B. Kasper, A. Kawai, K. Kopeckova, D.A. Krakorova, A. Le Cesne, F. Le Grange, E. Legius, A. Leithner, A. Lopez Pousa, J. Martin-Broto, O. Merimsky, C. Messiou, A.B. Miah, O. Mir, M. Montemurro, B. Morland, C. Morosi, E. Palmerini, M.A. Pantaleo, R. Piana, S. Piperno-Neumann, P. Reichardt, P. Rutkowski, A.A. Safwat, C. Sangalli, M. Sbaraglia, S. Scheipl, P. Schoffski, S. Sleijfer, D. Strauss, K. Sundby Hall, A. Trama, M. Unk, M.A.J. van de Sande, W.T.A. van der Graaf, W.J. van Houdt, T. Frebourg, R. Ladenstein, P.G. Casali, S. Stacchiotti, E.G. Esmo Guidelines Committee, E.R.N.P.E.a. clinicalguidelines@esmo.org, Bone sarcomas: ESMO-EURACAN-GENTURIS-ERN PaedCan Clinical Practice Guideline for diagnosis, treatment and follow-up, Ann Oncol 32(12) (2021) 1520–1536.

[7] O. Martin, B.M. Schaarschmidt, J. Kirchner, S. Suntharalingam, J. Grueneisen, A. Demircioglu, P. Heusch, H.H. Quick, M. Forsting, G. Antoch, K. Herrmann, L. Umutlu, PET/MRI Versus PET/CT for Whole-Body Staging: results from a Single-Center Observational Study on 1,003 Sequential Examinations, J. Nucl. Med. 61 (8) (2020) 1131–1136.

[8] I. Plaza de Las Heras, L. Garcia Canamaque, E. Quilez Caballero, M. Camacho-Arias, M.D.P. Cardenas Soriano, J. Martel Villagran, Positron emission tomography-magnetic resonance imaging applications in pediatric musculoskeletal tumors, Quant Imaging Med Surg 14(11) (2024) 7825–7838.

[9] L. Garcia Canamaque, C.A. Field, F.S. Furtado, D.E.L.H.I. Plaza, J.S. Husseini, R. Balza, M. Jarraya, O.A. Catalano, M. Mitjavila Casanovas, Contribution of positron emission tomography/magnetic resonance imaging in musculoskeletal malignancies, Q. J. Nucl. Med. Mol. Imaging 66 (1) (2022) 3–14.

[10] M. Chodyla, F. Barbato, U. Dirksen, J. Kirchner, B.M. Schaarschmidt, B. Schweiger, M. Forsting, K. Herrmann, L. Umutlu, J. Grueneisen, Utility of Integrated PET/MRI for the Primary Diagnostic Work-up of patients with Ewing Sarcoma: Preliminary results, Diagnostics (basel) 12 (10) (2022).

[11] F. Schmitz, H. Voigtlander, H. Jang, H.P. Schlemmer, H.U. Kauczor, S. Sedaghat, Predicting the Malignancy Grade of Soft Tissue Sarcomas on MRI using conventional image Reading and Radiomics, Diagnostics (basel) 14 (19) (2024).

[12] B. Akkus Yildirim, C. Onal, G. Erbay, O. Cem Guler, E. Karadeli, M. Reyhan, Z. Koc, Prognostic values of ADC(mean) and SUV(max) of the primary tumour in cervical cancer patients treated with definitive chemoradiotherapy, J. Obstet. Gynaecol. 39 (2) (2019) 224–230.

[13] M. Chodyla, A. Demircioglu, B.M. Schaarschmidt, S. Bertram, J. Morawitz, S. Bauer, L. Podleska, C. Rischpler, M. Forsting, K. Herrmann, L. Umutlu, J. Grueneisen, Evaluation of the Predictive potential of 18F-FDG PET and DWI Data Sets for Relevant Prognostic Parameters of Primary Soft-Tissue Sarcomas, Cancers (Basel) 13 (11) (2021).

[14] N.M. Bruckmann, J. Kirchner, J. Grueneisen, Y. Li, A. McCutcheon, C. Aigner, C. Rischpler, L.M. Sawicki, K. Herrmann, L. Umutlu, B.M. Schaarschmidt, Correlation of the apparent diffusion coefficient (ADC) and standardized uptake values (SUV) with overall survival in patients with primary non-small cell lung cancer (NSCLC) using (18)F-FDG PET/MRI, Eur. J. Radiol. 134 (2021) 109422.

[15] A.C. Guo, T.J. Cummings, R.C. Dash, J.M. Provenzale, Lymphomas and high-grade astrocytomas: comparison of water diffusibility and histologic characteristics, Radiology 224 (1) (2002) 177–183.

[16] R. Rakheja, H. Chandarana, L. DeMello, K. Jackson, C. Geppert, D. Faul, C. Glielmi, K.P. Friedman, Correlation between standardized uptake value and apparent diffusion coefficient of neoplastic lesions evaluated with whole-body simultaneous hybrid PET/MRI, AJR Am. J. Roentgenol. 201 (5) (2013) 1115–1119.

[17] B.M. Schaarschmidt, C. Buchbender, F. Nensa, J. Grueneisen, B. Gomez, J. Kohler, H. Reis, V. Ruhlmann, L. Umutlu, P. Heusch, Correlation of the apparent diffusion coefficient (ADC) with the standardized uptake value (SUV) in lymph node metastases of non-small cell lung cancer (NSCLC) patients using hybrid 18F-FDG PET/MRI, PLoS One 10 (1) (2015) e0116277.

[18] J.P. Hwang, I. Lim, B.H. Byun, B.I. Kim, C.W. Choi, S.M. Lim, Prognostic value of SUVmax measured by pretreatment 18F-FDG PET/CT in patients with primary gastric lymphoma, Nucl. Med. Commun. 37 (12) (2016) 1267–1272.

[19] D. Shi, G. Cai, J. Peng, D. Li, X. Li, Y. Xu, S. Cai, The preoperative SUVmax for (18) F-FDG uptake predicts survival in patients with colorectal cancer, BMC Cancer 15 (2015) 991.

[20] W. Diao, F. Tian, Z. Jia, The prognostic value of SUV(max) measuring on primary lesion and ALN by (18)F-FDG PET or PET/CT in patients with breast cancer, Eur. J. Radiol. 105 (2018) 1–7.

[21] R. Rakheja, W. Makis, S. Skamene, A. Nahal, F. Brimo, L. Azoulay, J. Assayag, R. Turcotte, M. Hickeson, Correlating metabolic activity on 18F-FDG PET/CT with histopathologic characteristics of osseous and soft-tissue sarcomas: a retrospective review of 136 patients, AJR Am. J. Roentgenol. 198 (6) (2012) 1409–1416.

[22] M. Chodyla, A. Demircioglu, B.M. Schaarschmidt, S. Bertram, N.M. Bruckmann, J. Haferkamp, Y. Li, S. Bauer, L. Podleska, C. Rischpler, M. Forsting, K. Herrmann, L. Umutlu, J. Grueneisen, Evaluation of (18)F-FDG PET and DWI Datasets for predicting Therapy Response of Soft-Tissue Sarcomas under Neoadjuvant Isolated Limb Perfusion, J. Nucl. Med. 62 (3) (2021) 348–353.

[23] O. Dudeck, M. Zeile, D. Pink, M. Pech, P.U. Tunn, P. Reichardt, W.D. Ludwig, B. Hamm, Diffusion-weighted magnetic resonance imaging allows monitoring of anticancer treatment effects in patients with soft-tissue sarcomas, J. Magn. Reson. Imaging 27 (5) (2008) 1109–1113.

[24] B.H. Byun, C.B. Kong, I. Lim, C.W. Choi, W.S. Song, W.H. Cho, D.G. Jeon, J.S. Koh, S.Y. Lee, S.M. Lim, Combination of 18F-FDG PET/CT and diffusion-weighted MR imaging as a predictor of histologic response to neoadjuvant chemotherapy: preliminary results in osteosarcoma, J. Nucl. Med. 54 (7) (2013) 1053–1059.

[25] B. Jamet, T. Carlier, L. Campion, E. Bompas, S. Girault, F. Borrely, L. Ferrer, M. Rousseau, Y. Venel, F. Kraeber-Bodere, C. Rousseau, Initial FDG-PET/CT predicts survival in adults Ewing sarcoma family of tumors, Oncotarget 8 (44) (2017) 77050–77060.

[26] G. El-Hennawy, H. Moustafa, W. Omar, N. Elkinaai, A. Kamel, I. Zaki, N. Farid, E. El-Kholy, Different (18) F-FDG PET parameters for the prediction of histological

response to neoadjuvant chemotherapy in pediatric Ewing sarcoma family of tumors, Pediatr. Blood Cancer 67 (11) (2020) e28605.
[27] A. Annovazzi, V. Ferraresi, V. Anelli, R. Covello, S. Vari, C. Zoccali, R. Biagini, R. Sciuto, [(18)F]FDG PET/CT quantitative parameters for the prediction of histological response to induction chemotherapy and clinical outcome in patients with localised bone and soft-tissue Ewing sarcoma, Eur. Radiol. 31 (9) (2021) 7012–7021.
[28] D. Albano, F. Dondi, R.F. Schumacher, C. D'Ippolito, F. Porta, R. Giubbini, F. Bertagna, Clinical and Prognostic Role of 18F-FDG PET/CT in Pediatric Ewing Sarcoma, J. Pediatr. Hematol. Oncol. 42 (2) (2020) e79–e86.
[29] M. Salzer-Kuntschik, G. Delling, G. Beron, R. Sigmund, Morphological grades of regression in osteosarcoma after polychemotherapy - study COSS 80, J. Cancer Res. Clin. Oncol. 106 (Suppl) (1983) 21–24.
[30] M. Hassanzad, K. Hajian-Tilaki, Methods of determining optimal cut-point of diagnostic biomarkers with application of clinical data in ROC analysis: an update review, BMC Med. Res. Methodol. 24 (1) (2024) 84.
[31] T. Robba, V. Chianca, D. Albano, V. Clementi, R. Piana, A. Linari, A. Comandone, G. Regis, M. Stratta, C. Faletti, A. Borre, Diffusion-weighted imaging for the cellularity assessment and matrix characterization of soft tissue tumour, Radiol. Med. 122 (11) (2017) 871–879.
[32] M. Ozturk, A.V. Polat, F.C. Tosun, M.B. Selcuk, Does the SUVmax of FDG-PET/CT Correlate with the ADC Values of DWI in Musculoskeletal Malignancies? J Belg Soc Radiol 105 (1) (2021) 11.
[33] D. Schnapauff, M. Zeile, M.B. Niederhagen, B. Fleige, P.U. Tunn, B. Hamm, O. Dudeck, Diffusion-weighted echo-planar magnetic resonance imaging for the assessment of tumor cellularity in patients with soft-tissue sarcomas, J. Magn. Reson. Imaging 29 (6) (2009) 1355–1359.
[34] E.C. Ehman, G.B. Johnson, J.E. Villanueva-Meyer, S. Cha, A.P. Leynes, P.E. Z. Larson, T.A. Hope, PET/MRI: where Might it Replace PET/CT? Journal of Magnetic Resonance Imaging : JMRI 46 (5) (2017 Mar 30).
[35] A.L. Folpe, R.H. Lyles, J.T. Sprouse, E.U. Conrad 3rd, J.F. Eary, (F-18) fluorodeoxyglucose positron emission tomography as a predictor of pathologic grade and other prognostic variables in bone and soft tissue sarcoma, Clin. Cancer Res. 6 (4) (2000) 1279–1287.
[36] J.F. Eary, E.U. Conrad, J.D. Bruckner, A. Folpe, K.J. Hunt, D.A. Mankoff, A. T. Howlett, Quantitative [F-18]fluorodeoxyglucose positron emission tomography in pretreatment and grading of sarcoma, Clin. Cancer Res. 4 (5) (1998) 1215–1220.
[37] C.S. Wong, N. Gong, Y.C. Chu, M.P. Anthony, Q. Chan, H.F. Lee, K.M. Chu, P. L. Khong, Correlation of measurements from diffusion weighted MR imaging and FDG PET/CT in GIST patients: ADC versus SUV, Eur. J. Radiol. 81 (9) (2012) 2122–2126.
[38] K. Herrmann, M.R. Benz, J. Czernin, M.S. Allen-Auerbach, W.D. Tap, S.M. Dry, T. Schuster, J.J. Eckardt, M.E. Phelps, W.A. Weber, F.C. Eilber, 18F-FDG-PET/CT Imaging as an early survival predictor in patients with primary high-grade soft tissue sarcomas undergoing neoadjuvant therapy, Clin. Cancer Res. 18 (7) (2012) 2024–2031.
[39] J. Grueneisen, B. Schaarschmidt, A. Demircioglu, M. Chodyla, O. Martin, S. Bertram, A. Wetter, S. Bauer, W.P. Fendler, L. Podleska, M. Forsting, K. Herrmann, L. Umutlu, (18)F-FDG PET/MRI for Therapy Response Assessment of Isolated Limb Perfusion in patients with Soft-Tissue Sarcomas, J. Nucl. Med. 60 (11) (2019) 1537–1542.
[40] A. A, F. V, A. V, C. R, V. S, Z. C, B. R, S. R, [18F]FDG PET/CT quantitative parameters for the prediction of histological response to induction chemotherapy and clinical outcome in patients with localised bone and soft-tissue Ewing sarcoma - PubMed, European radiology 31(9) (2021 Sep).
[41] E.-H. G, M. H, O. W, E. N, K. A, Z. I, F. N, E.-K. E, Different 18 F-FDG PET parameters for the prediction of histological response to neoadjuvant chemotherapy in pediatric Ewing sarcoma family of tumors - PubMed, Pediatric blood & cancer 67(11) (2020 Nov).
[42] J. B, C. T, C. L, B. E, G. S, B. F, F. L, R. M, V. Y, K.-B. F, R. C, Initial FDG-PET/CT predicts survival in adults Ewing sarcoma family of tumors - PubMed, Oncotarget 8 (44) (08/18/2017).
[43] D. AJ, C. CY, S. AJ, Quantitative diffusion-weighted magnetic resonance imaging assessment of chemotherapy treatment response of pediatric osteosarcoma and Ewing sarcoma malignant bone tumors - PubMed, Clinical imaging 47 (2018 Jan–Feb).
[44] J.C. Ho, P. Fang, C.E. Cardenas, A.S.R. Mohamed, C.D. Fuller, P.K. Allen, P. R. Bhosale, M.M. Frumovitz, A. Jhingran, A.H. Klopp, Volumetric assessment of apparent diffusion coefficient predicts outcome following chemoradiation for cervical cancer, Radiother. Oncol. 135 (2019) 58–64.
[45] G. Orsatti, P. Zucchetta, A. Varotto, F. Crimi, M. Weber, D. Cecchin, G. Bisogno, A. Spimpolo, C. Giraudo, R. Stramare, Volumetric histograms-based analysis of apparent diffusion coefficients and standard uptake values for the assessment of pediatric sarcoma at staging: preliminary results of a PET/MRI study, Radiol. Med. 126 (6) (2021) 878–885.